Kaon Production in the MiniBooNE Detector

Kiril Datchev

July 24, 2003

1 Introduction

Neutrino interactions at MiniBooNE resulting in strange quarks are energetically disfavored compared to final states containing only nucleons and pions, but over the course of the MiniBooNE data run there should still be a significant number of kaons. A measurement of the exact rate of kaon production is of particular interest to experiments looking for proton decay because these experiments face an irreducible background from atmospheric neutrinos, many of which fall in an energy range comparable to that of MiniBooNE. Some supersymmetric theories predict the possibility of a proton decaying into, for example, a kaon and a lepton at a very low rate, and this idea is being tested by a number of present and proposed nucleon decay experiments [1, 2, 3, 4, 5]. But atmospheric neutrinos interacting with protons could also produce kaons, thus mimicking the decay, and because these experiments cannot expect very large statistics, they need an especially solid understanding of these other sources.

2 Theoretical models

Table 1 shows a list of some of the major channels of kaon production at low energies, on the order of 1 GeV. Included are possible interactions which result in a lepton, a kaon and a baryon. Final states containing multiple mesons are omitted. The first three channels in the charged-current column are flavor changing; the other final states all contain both an s and $\bar{s}$ quark.

Charged Current	Neutral Current
$\nu_\mu p \to \mu^- K^+ p$	$\nu_\mu p \to \nu_\mu K^+ \Lambda^0$
$\nu_\mu n \to \mu^- K^0 p$	$\nu_\mu n \to \nu_\mu K^0 \Lambda^0$
$\nu_\mu n \to \mu^- K^+ n$	$\nu_\mu p \to \nu_\mu K^+ \Sigma^0$
$\nu_\mu n \to \mu^- K^+ \Lambda^0$	$\nu_\mu p \to \nu_\mu K^0 \Sigma^+$
$\nu_\mu p \to \mu^- K^+ \Sigma^+$	$\nu_\mu n \to \nu_\mu K^- \Sigma^+$
$\nu_\mu n \to \mu^- K^+ \Sigma^0$	$\nu_\mu n \to \nu_\mu K^+ \Sigma^-$
$\nu_\mu n \to \mu^- K^0 \Sigma^+$	$\nu_\mu n \to \nu_\mu K^0 \Sigma^0$

Table 1: Channels of kaon production at MiniBooNE

Neutrino-induced kaon production has not been investigated from a theoretical standpoint in much depth in the past. Robert E. Shrock estimated rates for processes resulting in a K and a Λ in a 1975 paper [6] using a nonresonant Born model, but the results do not fit the data very well and do not level off at high energies. The Shrock goal was only to give a rough idea of the cross-section [7], which he correctly predicted would be on the order of 10^{-40} cm^2. He draws a parallel with analogous calculations of rates for neutrino-induced pion production, where again models were largely unpredicitive until they could be tuned to measurements. In the case of single K production, the absence of experimental results measuring cross-sections has made further development of theoretical models difficult.

A. A. Amer also calculated cross-sections for the production of $K^+\Lambda^0$ in a 1977 paper [8], but using a model of neutrino production of resonances based on a harmonic oscillator quark model, while Shrock assumes only associated (nonresonant) production. Amer estimates the cross-section to be between 1.35 and 2.65 $\times 10^{-41}$ cm^2, but this is more than an order of magnitude below the measured rate of 4.7×10^{-40} cm^2 [9].

Using David Casper's cross-section calculating program Nuance [10], currently being used in MiniBooNE and also K2K, the the prediction in Figure 1 is obtained.

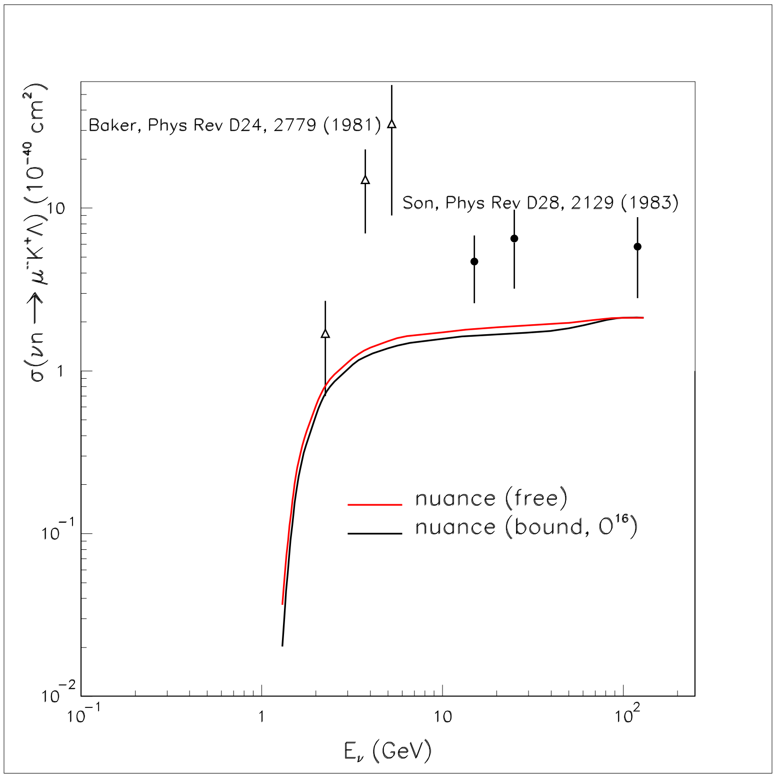

Figure 1: Data points with Nuance theoretical estimate for the channel $\nu_\mu n \to \mu^- K^+ \Lambda^0$

This estimate misses the data points by a factor of four and has an overall χ^2 of 11/6, but the program includes only resonant kaon production based on the Rein and Sehgal models for pion production [11, 12]. Table 2 lists the various resonances included in the model which can result in $K^+\Lambda^0$ final states, as well as the branching ratios both from the program [10] and from the Particle Data Group [13].

Resonance	Branching Ratio	
	Nuance Program	Particle Data Group
$N(1650)$	8%	3–11%
$N(1675)$	0%	<1%
$N(1700)$	0%	<3%
$N(1710)$	15%	5–25%
$N(1720)$	5%	1–15%
$N(1970)$	10%	resonance not listed

Table 2: Resonances with branching ratios for final state $K^+\Lambda^0$

If one includes deep inelastic processes in the model, which are simulated beginning at an energy of 2.2 GeV, the fit is improved somewhat, but this does not help the situation at lower energies. This is shown in figure 2. Even with this correction, however, Nuance still does not model flavor-changing charged current channels such as $\nu_\mu p \to \mu^- K^+ p$

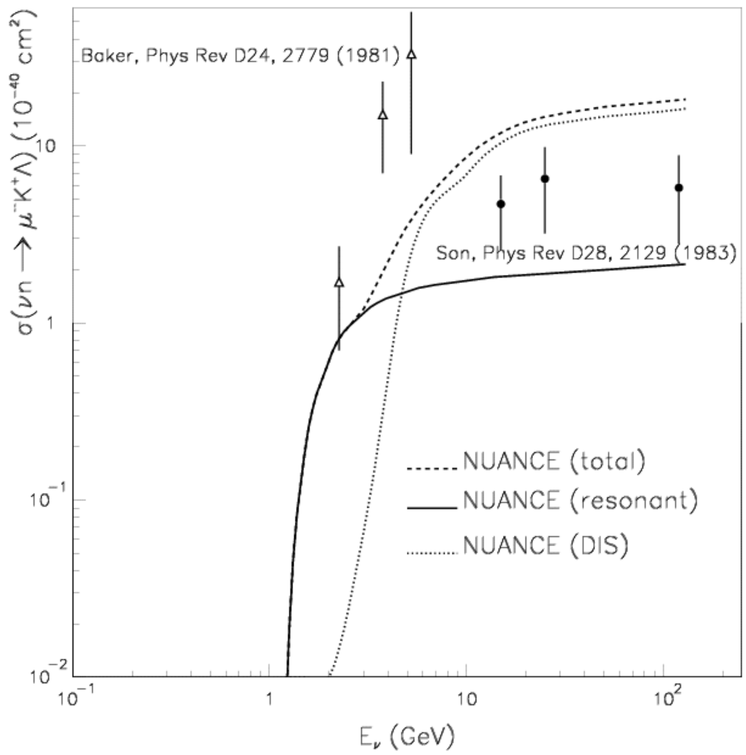

Figure 2: Data points with Nuance theoretical estimate for the channel $\nu_\mu n \to \mu^- K^+\Lambda^0$ including deep inelastic processes

3 Preliminary cross-section estimates

Most experimental information about these cross-sections in our energy range dates back to bubble chamber experiments from the 70s and 80s [9, 14, 15]. As a result the most studied channel has been $\nu_\mu n \to \mu^- K^+ \Lambda^0$ because it is the easiest way to produce a Λ^0 and these particles are easily recognized in a bubble chamber. Because of the disparities between the different theoretical models available for this type of process a fitted curve to the data points from previous measurements is used to predict the number of events in MiniBooNE (see Figure 3). The curve is an error function modified to give a threshold of 1.1 GeV while passing through the first data point and asymptotically approaching an appropriate level. It has a χ^2 value of 3.81/6.

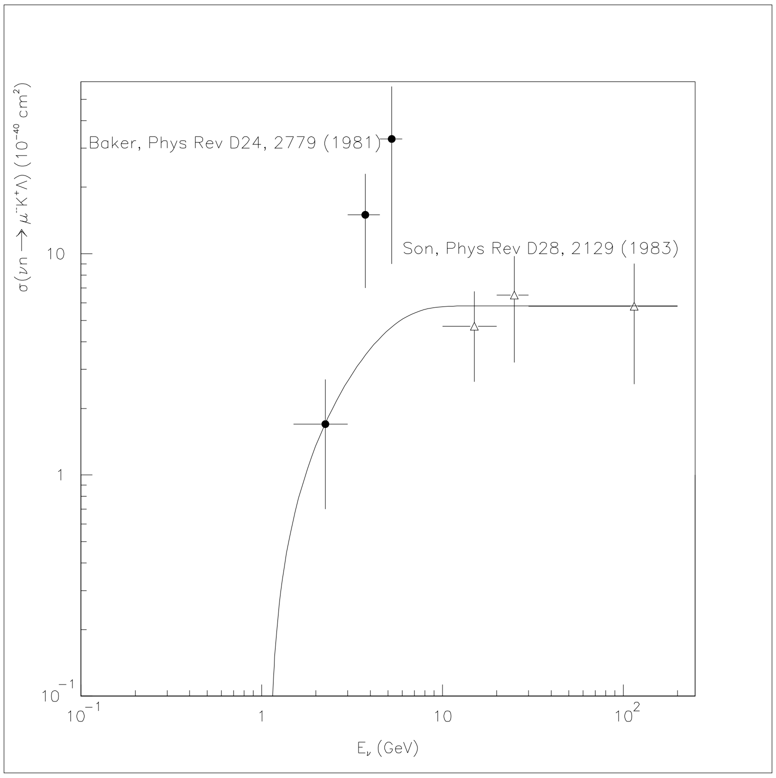

Figure 3: Data points with fitted curve for the channel $\nu_\mu n \to \mu^- K^+ \Lambda^0$

This is the most investigated channel, and the cross-sections for other channels are approximated using the same basic shape for the curve, multiplying by appropriate scaling factors to get the relative rates right, and then shifting the curve over to adjust the thresholds.

The cross-section for $\nu_\mu n \to \mu^- K^+ \Lambda^0$ levels off at around 6×10^{-40} cm^2. The equivalent neutral current interactions ($\nu_\mu n \to \nu_\mu K^0 \Lambda^0$ and $\nu_\mu p \to \nu_\mu K^+ \Lambda^0$) resulting in Λ^0s should each have about one quarter that cross-section. Because these last two interactions are so similar, their cross-sections should be approximately equal [2, 6, 14]. Similarly the three flavor changing charged current interactions which result in nucleons should all have about the same cross section. Each of these processes can be realized in two basic ways, either by scattering off of a $\bar{u}$ quark in the sea or else by scattering off an s quark in the sea. The Cabibbo suppression factor associated with the process $d \to u$ in the interaction $\nu_\mu p \to \mu^- \pi^+ p$ is $(.9754)^2$, while the factor for the processes $\bar{u} \to \bar{s}$ and $s \to u$ in the flavor changing channels is $(.2205)^2$. The pion production channel has been extensively measured and that cross section levels off at around 70×10^{-40} cm^2 [16]. This suggests that the three flavor changing channels should each have a cross-section of about 5.5% of that for $\nu_\mu p \to \mu^- \pi^+ p$ for both the $s \to d$ and $\bar{u} \to \bar{s}$. This latter channel is further suppressed by helicity considerations, making its cross-section one third that of the former one. Furthermore pion production is dominated by resonant production, while there are no known resonances which can result in a kaon and a nucleon [13]. The ratio of the rates for $\nu_\mu p \to \mu^- K^+ p$ to $\nu_\mu p \to \mu^- \pi^+ p$ has been measured to be around 1.7% [17]. So the actual ratio is smaller than one would expect from Cabibbo considerations alone, but this is largely because of the fact that resonances dominate the pion production channels but not the kaon production channels. So the cross-sections for these flavor changing processes should each be about equal and level off at 1.2×10^{-40} cm^2. Figure 4 shows a plot of each of these rates around MiniBooNE's energy range.

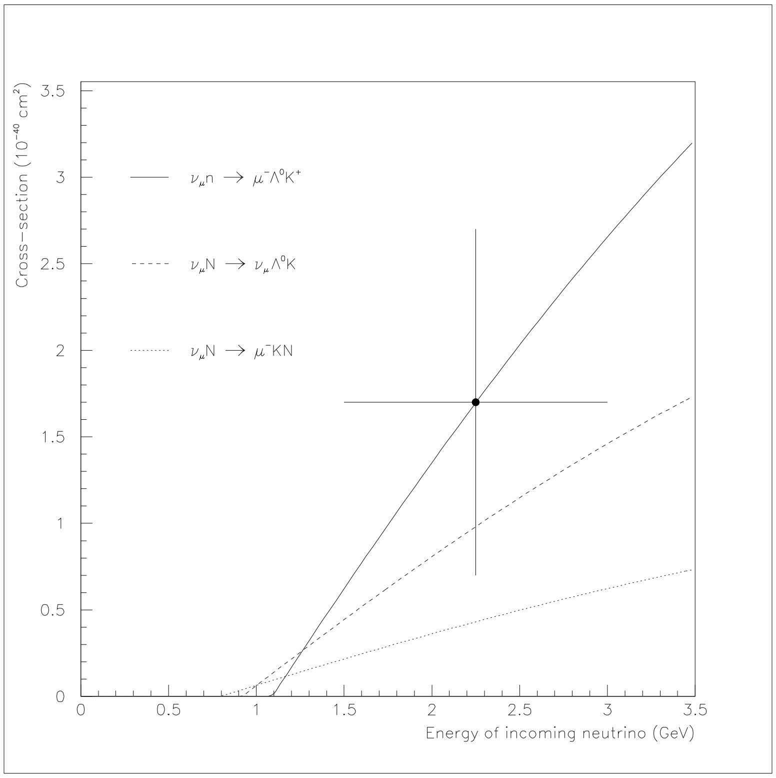

Figure 4: Estimated cross-sections for probable neutrino-nucleon interactions. Data point is from N. J. Baker *et al.*, Phys. Rev. D **24**, 2779 (1981).

4 Event rates at MiniBooNE

Convoluting this with the MARS flux estimate for MiniBooNE (Figure 5) and assuming a fiducial detector of 450 tons (4.04×10^8 grams) gives the event rates shown in Table 3. These all assume 5×10^{20} protons on target (expected by the end of the MiniBooNE run) and a detection efficiency of 100%. One bubble chamber experiment using a somewhat similar neutrino energy spectrum cites event rates for the processes $\nu_\mu n \to \mu^- K^+ \Lambda^0$ and $\nu_\mu p \to \mu^- K^+ p$ which are comparable, whereas according to these estimates the $K^+\Lambda^0$ is expected to dominate, but their results are quoted with large errors [2].

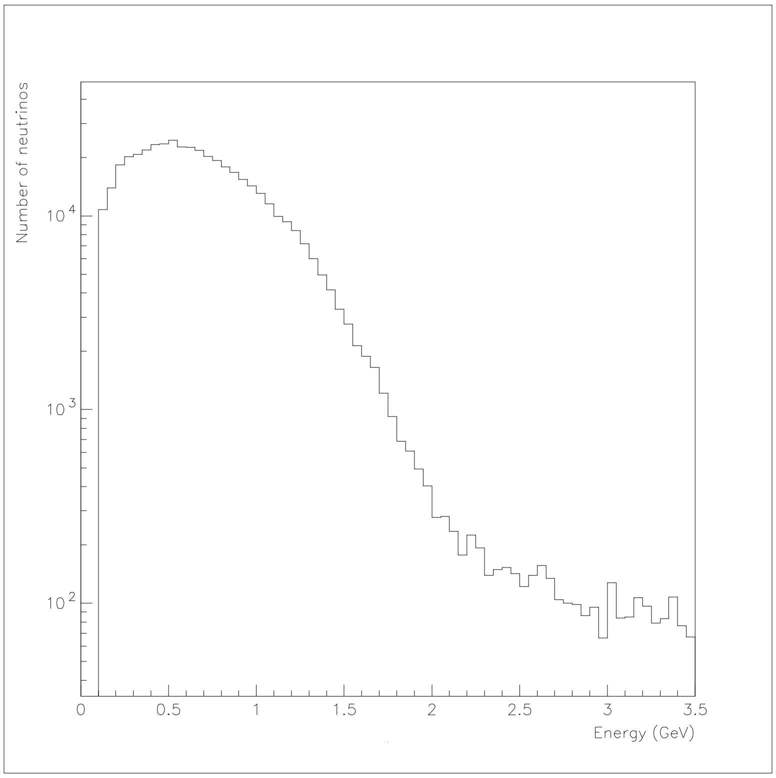

Figure 5: MARS ν_μ flux estimate for 6 billion protons on target

Channel	Events
$\nu_\mu n \to \mu^- K^+ \Lambda^0$	143
$\nu_\mu p \to \mu^- K^+ p$	122
$\nu_\mu n \to \mu^- K^0 p$	91
$\nu_\mu n \to \mu^- K^+ n$	91
$\nu_\mu p \to \nu_\mu K^+ \Lambda^0$	83
$\nu_\mu n \to \nu_\mu K^0 \Lambda^0$	62

Table 3: Estimated event rates for major kaon-production channels assuming 100% efficiency and MARS flux model

Altogether there will be about 439 K^+s produced and 153 K^0s, not counting events which result in Σ baryons or events which result in multiple mesons. These channels have not been investigated in much detail in the past, but they are suppressed in the MiniBooNE energy range and will in any case only add events. By comparison the bubble chamber experiments from the 70s and 80s had event rates on the order of a few dozen at most. It is also possible that these cross-sections are too optimistic. The fit for $\nu_\mu n \to \mu^- K^+ \Lambda^0$ is almost linear between the threshold and the first data point, which is at 2.25 GeV, but most of the events at MiniBooNE will be at lower and relatively uncharted energies, and this data point itself has large errors. More significant mass suppression effects may cause the cross section to increase a great deal more slowly than anticipated, but there should still be events even if this effect is of two orders of magnitude.

It should be emphasized that overall there is very little theoretical or experimental guidance for estimating these cross-sections, so the event rates listed here are necessarily only rough estimates about what MiniBooNE can hope to see.

5 Monte Carlo predictions of kaon properties

Not all of the particles produced will be detected. A K^+ decays 63.5% of the time to $\mu^+\nu_\mu$ and 21.2% of the time to $\pi^+\pi^0$ [13]. Because most kaon production will occur near threshold, the majority of the K^+s will have low kinetic energies and will come to a stop by interacting electromagnetically before they decay. The resultant two body decays will then produce a monoenergetic stream of μ^+s which can be seen by the detector [18].

Separating individual channels of K^+ production will probably be difficult. It will certainly be possible to distinguish charged current and neutral current events, but identifying the accompanying baryons is likely to prove more problematic Λ baryons decay 63.9% of the time to $p\pi^-$, and 35.8% of the time to $n\pi^0$. π^-s in our detector will be practically invisible, because they will generally be captured quickly by nearby nuclei, but it may be possible to see the π^0s [18].

A sample of 10 million Nuance neutrino events gathered from 200 files of 50000 events each was examined for kaons, and 1979 events were found to contain one or more K^+s. These were stripped out from the original samples and spliced together into a single file, and then simulated in the BooDetMC model of the MiniBooNE detector, and the momentum distributions in Figure 6 came about.

The kaons tend to be high momentum: nearly two-thirds are above the Cherenkov threshold of 0.453 GeV. However, in spite of this, practically all of them stop electromagnetically before they decay. The plot of μ^+ momentum distributions shows that almost all the muons fall into two energy bins. One group corresponds to the 153 MeV kinetic energy muon produced by a kaon decay-at-rest, and the other group corresponds to the lower-energy monoenergetic muon which comes about as a result of a π^+ decay when the kaon decays via $\pi^+\pi^0$ rather than $\mu^+\nu_\mu$.

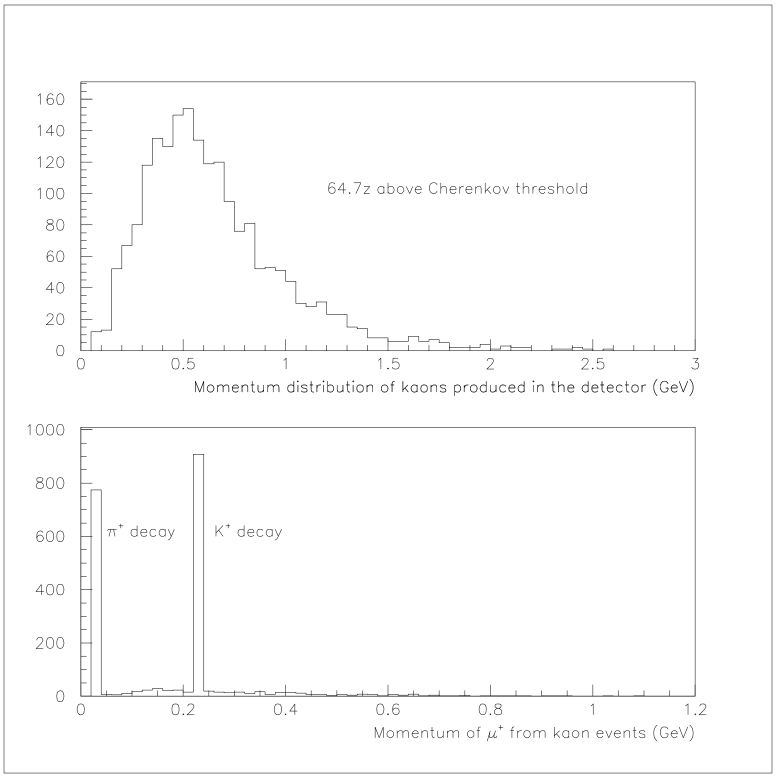

Figure 6: Results of Monte Carlo Simulations of Kaon Events

6 Preliminary cuts

One way to look for charged-current kaon production is to look for two michel electrons. One will come from the decay of the primary muon, and the other from the decay of the daughter of the K^+ or of the π^+ to which the K^+ decayed. To obtain an idea of what michel electrons look like in the detector a michel sample was generated by producing muons at the center of the tank and observing their decay properties (Figure 7). For this part of the Monte Carlo analysis, the approximation was made that any e^+ or e^- found in the tank was a Michel, which is true to 95% accuracy.

These plots suggest a cut for michels of tank hits between 20 and 150, and less than six veto hits to make sure the particle is from within the detector, as well as a demand that the subevent number be greater than one to insure that the particle is not a result of a primary neutrino interaction. These three cuts (20<THits<150, VHits<6, Subevent>1) were found to be 90% accurate at picking out michel electrons in a 10000 event sample of Nuance ν_μ events.

Kaon events tend to be of higher average energy than other events (Figure 8) so this two Michel cut was coupled with a cut on Tank Hits > 600 in the first subevent. These cuts had the following effect on the general and kaon data samples (Figure 9). After these cuts one is left with background reduced by two orders of magnitude while the signal is reduced to 20.2% of what it was before. This last number is in some ways deceptively low, because 1/4

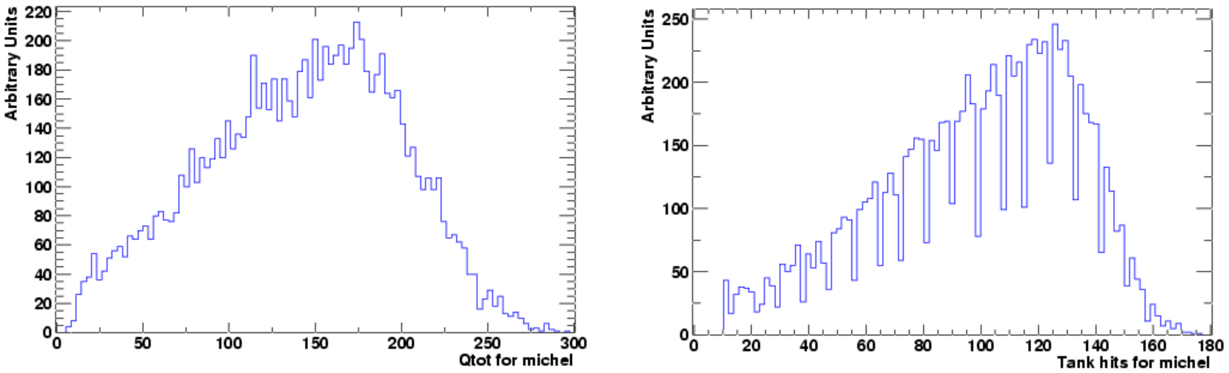

Figure 7: Tank hits and total charge for michels in the detector

of the original K^+ event sample consisted of neutral current events, which such a cut explicitly selects against. This still leaves a background to signal ratio of 165:2, so much more efficient cuts are needed. By far the dominant remaining background is from the process $\nu_\mu p \to \mu^- \pi^+ p$, where a high energy pion event can look like a kaon event.

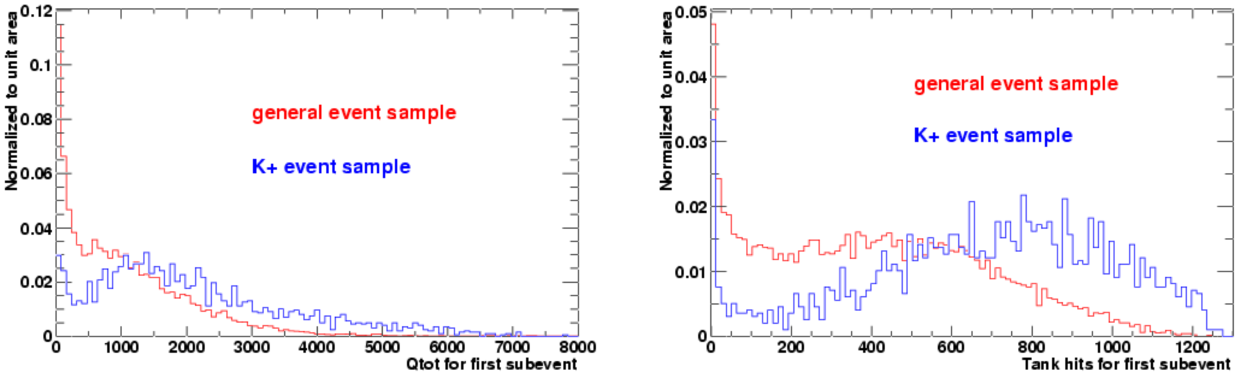

Figure 8: Comparison of total charge and tank hits in first subevent

7 Tracking the monoenergetic muon signal

The best way to eliminate the background on kaon production should be the detection of the 153 MeV decay muon which appears after the primary event, when the kaon decays. This is tricky for a number of reasons. First of all it requires a precise timing cut where effects on the scale of a few nanoseconds, such as the time of flight of a Cherenkov photon to reach the PMT, are critical. The muon must be separated enough in time to be distinguishable from the primary event, yet at the same time its prompt light must also be distinguishable from the scintillation light of the primary event. This leaves one with the daunting tasks of

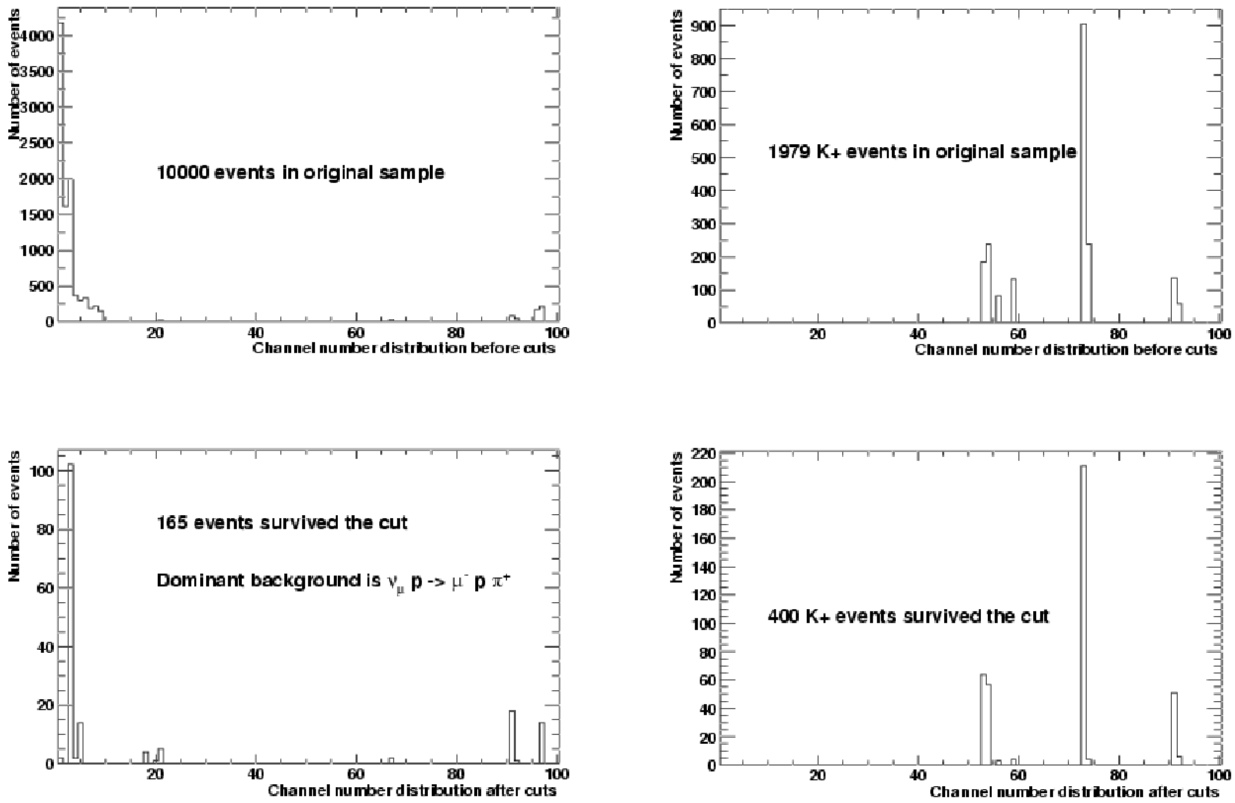

Figure 9: Effect of two michel and >600 tank hits cut on general sample(left) and kaon sample(right)

first separating out the muon into its own subevent and then fitting it into a background of concurrent scintillation light and already hit PMTs from the primary event.

One way to look for such elusive muons is using the Hough Transform. This is a technique for looking for straight edges in events which has been modified to look for rings, and it has claims of being exceptionally robust against noise, which is a special obstacle in this analysis [19]. Figure 10 shows six such muons generated at random places in the tank. The plots are in $cos\theta$ vs ϕ space. The different colors indicate the intensity of the transformed hits, while the black crosses indicate the positions of the original hits. While the narrow peaks are irregular, looked at broadly in terms of the wide light blue peaks they are of approximately equal width. Looking for these muons in the context of a messy kaon event will be more difficult, but perhaps the Hough transform technique could still be useful.

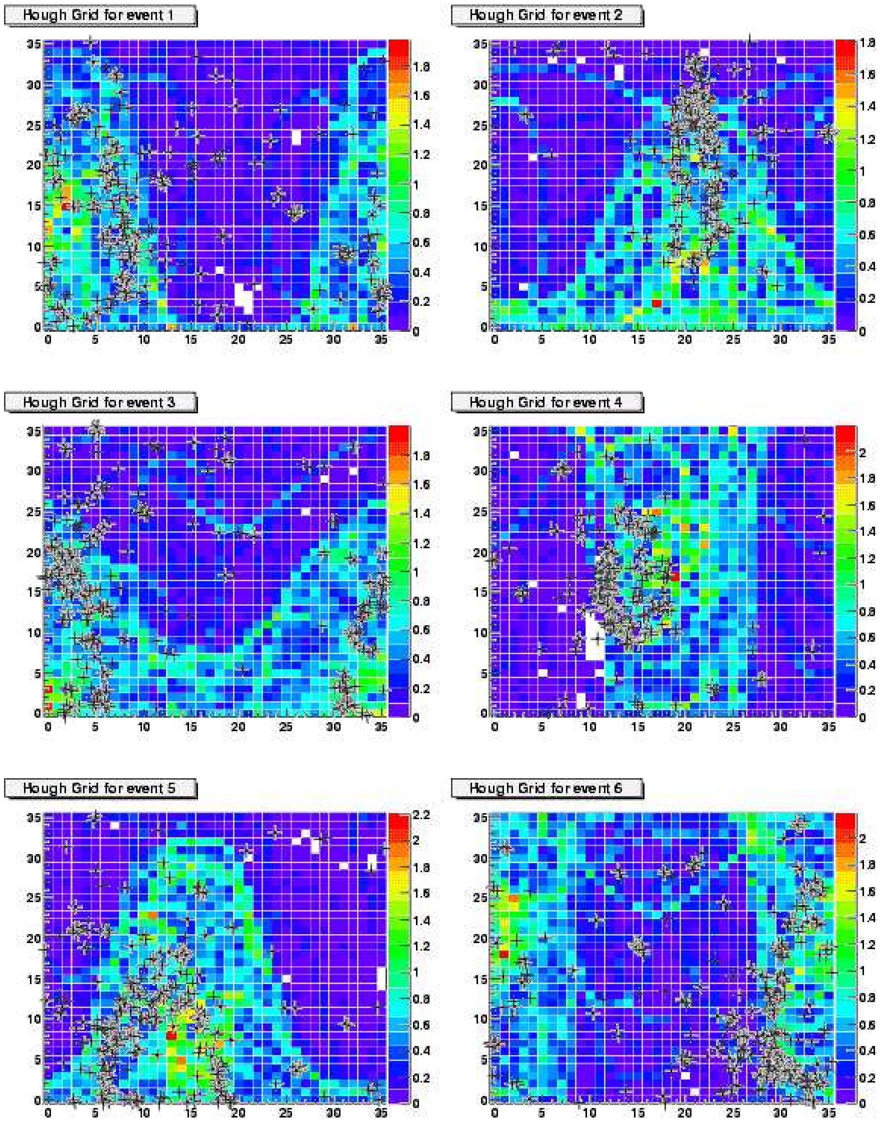

Figure 10: 153 MeV muon events analyzed under the Hough Transform

References

[1] Y. Hayato *et al.* [SuperKamiokande Collaboration], "Search for proton decay through p $\rightarrow$ anti-nu K+ in a large water Cherenkov detector," Phys. Rev. Lett. **83**, 1529 (1999) [arXiv:hep-ex/9904020].

[2] W. A. Mann, T. Kafka, M. Derrick, B. Musgrave, R. Ammar, D. Day and J. Gress, "K Meson Production By Muon-Neutrino - Deuterium Reactions Near Threshold: Implications For Nucleon Decay Searches," Phys. Rev. D **34**, 2545 (1986).

[3] Y. Suzuki *et al.* [TITAND Working Group Collaboration], "Multi-megaton water Cherenkov detector for a proton decay search: TITAND (former name: TITANIC)," arXiv:hep-ex/0110005.

[4] B. Viren [SuperKamiokande Collaboration], "Current status of nucleon decay searches with Super-Kamiokande," arXiv:hep-ex/9903029.

[5] M. A. Earl, "A Search For Nucleon Decay Into Modes Favored By Supersymmetry Using Superkamiokande," UMI-99-65646.

[6] R. E. Shrock, "Associated Production By Weak Charged And Neutral Currents," Phys. Rev. D **12**, 2049 (1975).

[7] R. E. Shrock, Personal Communication.

[8] A. A. Amer, "Production Of Strange Particles By Neutrinos And Anti-Neutrinos," Phys. Rev. D **18**, 2290 (1978).

[9] D. Son *et al.*, "Quasielastic Charmed Baryon Production And Exclusive Strange Particle Production By High-Energy Neutrinos," Phys. Rev. D **28**, 2129 (1983).

[10] D. Casper, proceedings of the NuInt01 workshop, http://neutrino.kek.jp/nuint01/

[11] D. Rein and L. M. Sehgal, "Neutrino Excitation Of Baryon Resonances And Single Pion Production," Annals Phys. **133**, 79 (1981).

[12] D. Rein, "Angular Distribution In Neutrino Induced Single Pion Production Processes," Z. Phys. C **35**, 43 (1987).

[13] D. E. Groom *et al.* [Particle Data Group Collaboration], "Review Of Particle Physics," Eur. Phys. J. C **15**, 1 (2000).

[14] N. J. Baker *et al.*, "Strange Particle Production From Neutrino Interactions In The Bnl 7-Ft Bubble Chamber," Phys. Rev. D **24**, 2779 (1981).

[15] S. J. Barish *et al.*, "Strange - Particle Production In Neutrino Interactions," Phys. Rev. Lett. **33**, 1446 (1974).

[16] H. M. Gallagher and M. C. Goodman, "Neutrino Cross Sections," NuMI-112 (1995).

[17] J. Bell *et al.*, "Cross-Section Measurements For The Reactions Neutrino P $\rightarrow$ Mu- Pi+ P And Neutrino P $\rightarrow$ Mu- K+ P At High-Energies," Phys. Rev. Lett. **41**, 1008 (1978).

[18] R. Imlay, "Measuring Inelastic Processes at MiniBooNE," MiniBooNE Internal Tech Note 60, July 2002.

[19] J. Raaf, "FHoughTransform" MiniBooNE Analysis Framework Users Manual, June 2003.